Single-Voxel Recording of Voltage Transients in Dendritic Spines – Supplemental Material

Corey D. Acker, Ping Yan, Leslie M. Loew
Center for Cell Analysis and Modeling, University of Connecticut Health Center, 400 Farmington Ave., Farmington CT. USA

Single-voxel, 2-photon recordings

To record from individual spines, we used a spot recording technique (1), which was synchronized to the electrical stimulation with sampling at 10 kHz. Because 2-photon excitation restricts the extent of excitation in the vertical dimension, we term this "single-voxel" recording. ScanImage, (MATLAB based, 2) was used to acquire images of regions with visible spines. Pixel times for frames were typically 3.2 μs and PMT signals were low-pass filtered with a filter cutoff of 300 kHz. Custom software was written (VoxelRecordVSD.m, Supplemental Materials) to select targets from these frames, position the laser at the selected location, and record PMT signals for a given duration (typically 40-60 ms). While recording from single voxels, the software automatically switched the low-pass filter cutoff from 300 kHz to 3 kHz (serial communication with Stanford Research SR570). Signals were sampled at 1 MHz and decimated (downsampled) twice by a factor of 10 to reduce the sampling to 10 kHz. Additional 3 kHz filtering was built into the decimation software, and "zero-phase" filtering (filtfilt, MATLAB) was used to preserve signal timing, allowing us to accurately measure propagation delays of backpropagating action potentials traveling from soma to dendrite. Control data was first high pass filtered at 100 Hz before taking the standard deviation when computing signal-to-noise.

Custom 2-photon microscope and optics

A Zeiss AxioSkop 2FS MOT was modified for 2-photon as follows. A 40X 1.0NA water objective (Zeiss, W Plan-Apochromat 1.0) was used for excitation. A transfluorescence light path was added using a 1.2NA water immersion condenser (Zeiss) coupled to a PMT. PMTs were Hamamatsu GaAs(P) (H10770PA-40). The Ti:Sapphire laser was a Coherent Chameleon Ultra II, with an electro-optic modulator (Conoptics Model 350-80LA with BK option), and scanning was performed with Cambridge Technology galvanometers (6215(y) and 6215H(x)). Excitation and epifluorescence light was separated by a 735 nm long-pass dichroic (Semrock FF01 735-Di01) and 640/120 nm emission filters were used (Chroma HQ 640/120 M 2P).

Brain slice electrophysiology

Acute brain slices were prepared from p24-p28 CD1 mice as described previously (3). Intracellular solution contained (in mM) 135 K-gluconate, 2 $MgCl_2$, 2 Mg-ATP, 10 Na-phosphocreatine, 0.3 Na-GTP, 10 HEPES, and 0.01 EGTA (pH 7.4, adjusted with KOH). ACSF contained (in mM) 127 NaCl, 25 NaHCO3, 25 D-glucose, 2.5 KCl, 1.25 NaH_2PO_4, 2 $CaCl_2$, and 1 $MgCl_2$ (pH 7.3). All recordings done at room temperature.

Dye loading and visualization of dendritic arbor

Using previously established techniques for loading similar voltage-sensitive dyes into neurons via a somatic whole-cell patch pipette, we were able to visualize apical dendritic trees of cortical pyramidal neurons in brain slice preparations with di-2-AN(F)EPPTEA. As previously described, "repatching" was necessary to allow the dye to diffuse sufficiently to distal dendritic regions (4). For the neuron shown in Fig. 2A (main paper), dye was allowed to diffuse for 35 minutes before repatching the neuron with a dye-free pipette.

Synthesis of di-2-AN(F)EPPTEA

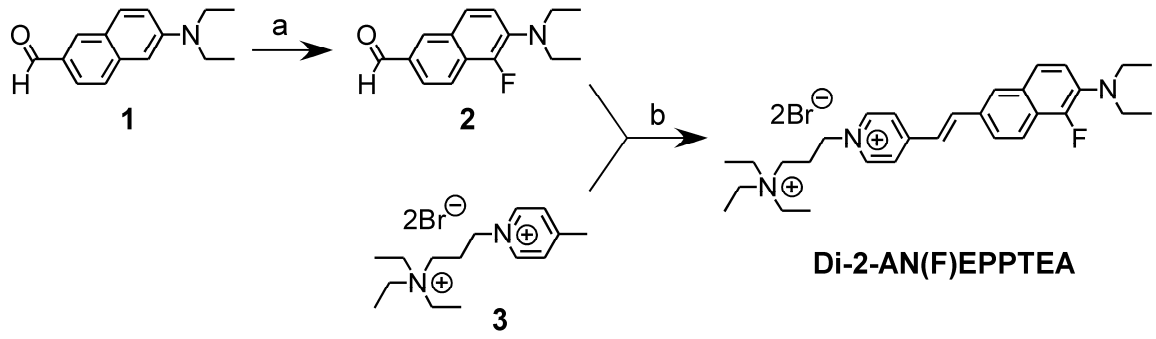

General.
6-Diethylamino-naphthalene-2-carboxaldehyde (**1**) and 1-(3-triethylammoniopropyl)-4-methylpyridinium dibromide (**3**) were synthesized according to the literature procedures (5, 6). Column chromatography for Di-2-AN(F)EPPTEA was performed on Unibond Amino silica gel from Analtech.

6-Diethylamino-5-fluoro-naphthalene-2-carboxaldehyde (2).
N-fluorobenzenesulfonimide (57.0 mg, 0.18 mmol) was added to a solution of 6-diethylamino-naphthalene-2-carboxaldehyde (**1,** 40.0 mg, 0.18 mmol) in 5 ml of anhydrous DMF under argon at -40 ^{o}C. The mixture was allowed to warm up to room temperature slowly. After 3 h, 10 mL of 10% K_2CO_3 (aq) solution was added and the product was extracted with ethyl acetate (3 × 50 mL). Solvent was removed by rotary evaporation and the residue was purified by chromatography (SiO_2, 1:1 hexane/CH_2Cl_2) to give **2** as yellow needles (35.0 mg, 79%). R_f (silica gel, 1:1 Hex/CH_2Cl_2) = 0.74; ^{1}H NMR (400 MHz, $CDCl_3$) δ 1.21 (t, *J* = 7.0 Hz, 6 H), 3.45 (q, *J* = 7.0 Hz, 4 H), 7.25 (t, *J* = 8.8 Hz, 1 H), 7.65 (d, *J* = 8.8 Hz, 1 H), 7.89 (dd, *J* = 1.2 Hz, 8.8 Hz, 1 H), 8.00 (d, *J* = 8.8 Hz, 1 H), 8.19 (s, 1 H), 10.06 (s, 1 H).

Di-2-AN(F)EPPTEA.
6-Diethylamino-5-fluoro-naphthalene-2-carboxaldehyde (**2**, 16 mg, 66 μmol) and 1-(3-triethylammoniopropyl)-4-methylpyridinium dibromide (**3**, 26 mg, 66 μmol) were mixed in 2 ml of ethanol, and then two drops of pyrrolidine was added. The solution was stirred at room temperature for 16 h and it turned red after reaction. Solvent was removed by rotary evaporation and the residue was purified by chromatography (SiO_2-amino, 5:95 MeOH/CH_2Cl_2) to give a red solid (16.4 mg, 40%). R_f (silica gel, 24:4:16:6:6 $CHCl_3$/i-PrOH/MeOH/H_2O/AcOH) = 0.26; ^{1}H NMR (400 MHz, CD_3OD) δ 1.18 (t, *J* = 7.2 Hz, 6 H), 1.35 (t, *J* = 7.0 Hz, 9 H), 2.50 (m, 2 H), 3.36–3.50 (m, 12 H), 4.68 (t, *J* = 7.6 Hz, 2 H), 7.36 (t, *J* = 8.8 Hz, 1 H), 7.52 (d, *J* = 16.0 Hz, 1 H), 7.67 (d, *J* = 8.8 Hz, 1 H), 7.91 (dd, *J* = 1.2 Hz, 8.8 Hz), 7.98 (d, *J* = 8.8 Hz, 1 H), 8.09 (s, 1 H), 8.12 (d, *J* = 16.0 Hz, 1 H), 8.25 (d, *J* = 6.4 Hz, 2 H), 8.93 (d, *J* = 6.4 Hz, 2 H); HRMS (FAB+): m/z = 542.2548 $[M-Br]^+$ (calcd for $C_{30}H_{42}BrFN_3^+$: 542.2546).

bAP waveforms in spines and their parent dendrite

When we recorded from parent dendrites near the spines, we confirmed the results of Holthoff, Zecevic and Konnerth (2010) and see nearly identical waveforms in spine and parent dendrite (Supplemental Figure 1). This effect persisted in spite of significantly narrower bAPs in the apical oblique dendrite than recorded previously in apical dendrites (7), with rise times of approximately 0.5 ms (Supplemental Figure 1E) and widths of approximately 1.0 ms (main Fig. 2G, Oblique). These results lend further support to the conclusion that bAPs fully invade spines from the adjacent dendrite (1, 7, 8). Interestingly, parent dendrites typically produced reduced signal amplitudes, with approximately two thirds the amplitude recorded in the spine (in % ΔF/F, Supplemental Figure 1C). This is most likely due to the bright internal staining of dendrites compared to spines, which adds background to the measurements.

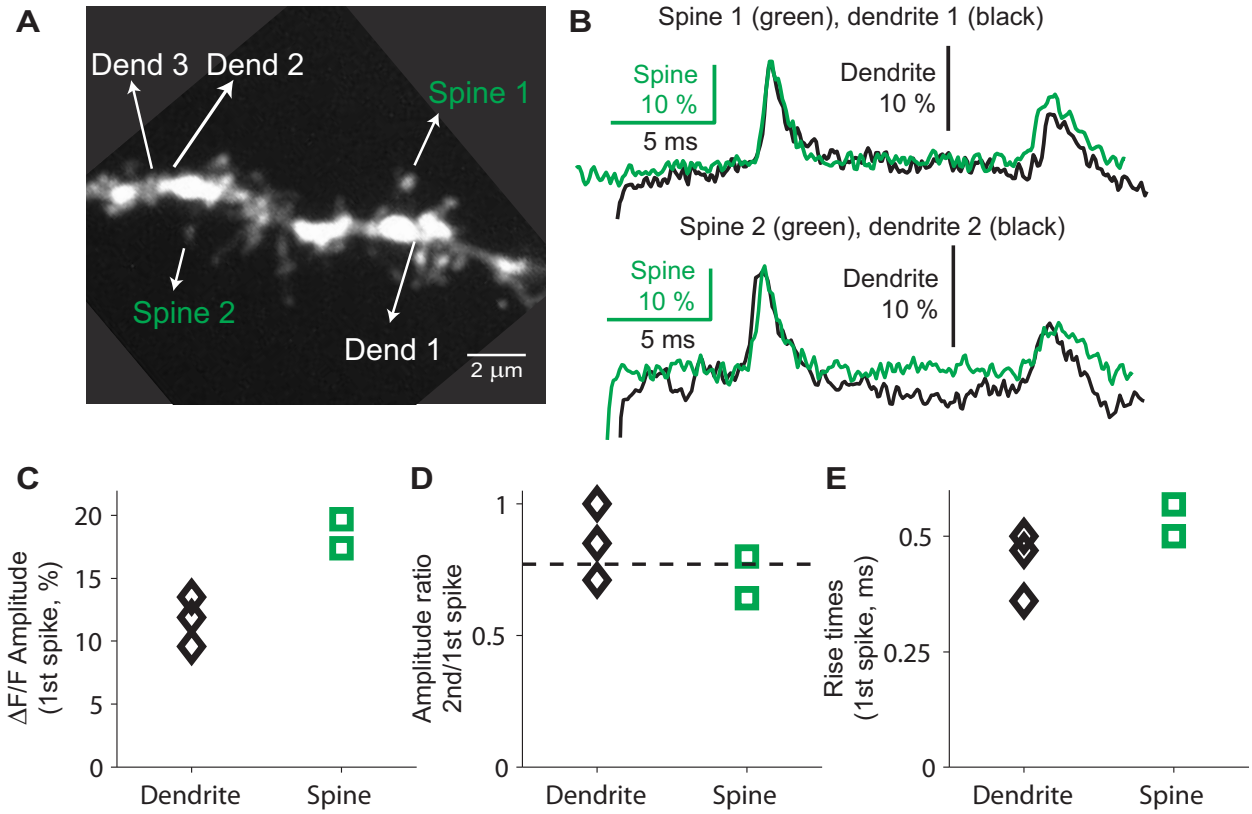

Supplemental Figure 1. bAP waveforms in spines and their parent dendrites. A. Apical oblique dendrite region (same as Fig 2B) with 2 spine and 3 dendrite recording sites labeled. B. Superimposed recordings from spines (green) and parent dendrite (black), notice different vertical scale bar for spines and dendrites. Somatic current injection generates 2 spikes, waveforms are averages (8-10 sweeps) aligned by first spike. C. Amplitudes of optically recorded bAPs (first spikes only). D. Ratio of second spike amplitudes over first, with the somatic value shown by the dashed line (0.77). E. Rise times of all first spikes.

Phototoxicity by intense somatic excitation

Since recording bAPs at single spines did not produce noticeable signs of phototoxicity such as changes in action potential shape (Fig. 1C) we developed a more extreme protocol targeted to the soma rather than spines. We rapidly and repeatedly scanned the soma (~1s/scan) with increasingly intense excitation light and looked for changes in action potential shape. 920nm was

used rather than 1060nm, which leads to approximately 10 times more excitation of the dye (Fig. 1B). The changes in somatic action potential shape typically included a ~30% increase in AP half width, ~15mV depolarization in resting membrane potential, and a ~15mV decrease in peak action potential amplitude. These changes developed gradually over ~100 exposures. Detectors were off during these measurements to prevent saturation or possible damage. Typically, 10-20mW of average power at 920nm was necessary to cause the above described changes. Further quantification is not feasible however, since the necessary laser power was clearly dependent on the depth of the cell in the slice (laser powers are accurate above slice only), with the deepest cell developing less noticeable changes with even higher powers.

References

1. Nuriya, M., J. Jiang, B. Nemet, K. Eisenthal, and R. Yuste. 2006. Imaging membrane potential in dendritic spines. Proceedings of the National Academy of Sciences of the United States of America:786-790.
2. Pologruto, T. A., B. L. Sabatini, and K. Svoboda. 2003. ScanImage: flexible software for operating laser scanning microscopes. Biomed Eng Online 2:13.
3. Acker, C. D., and S. D. Antic. 2009. Quantitative assessment of the distributions of membrane conductances involved in action potential backpropagation along basal dendrites. J Neurophysiol 101:1524-1541.
4. Antic, S. D. 2003. Action potentials in basal and oblique dendrites of rat neocortical pyramidal neurons. Journal of Physiology-London 550:35-50.
5. Wang, H., Z. Lu, S. Lord, K. Willets, J. Bertke, S. Bunge, W. Moerner, and R. Twieg. 2007. The influence of tetrahydroquinoline rings in dicyanomethylenedihydrofuran (DCDHF) single-molecule fluorophores. Tetrahedron:103-114.
6. Yan, P., A. Xie, M. Wei, and L. Loew. 2008. Amino(oligo)thiophene-based environmentally sensitive biomembrane chromophores. Journal of Organic Chemistry:6587-6594.
7. Holthoff, K., D. Zecevic, and A. Konnerth. 2010. Rapid time course of action potentials in spines and remote dendrites of mouse visual cortex neurons. Journal of Physiology-London 588:1085-1096.
8. Palmer, L. M., and G. J. Stuart. 2009. Membrane Potential Changes in Dendritic Spines during Action Potentials and Synaptic Input. Journal of Neuroscience 29:6897-6903.